3rd Quarterly Progress Report

May1 to July 31, 2003

Neural Prosthesis Program Contract N01-DC-02-1006

The Neurophysiological Effects of Simulated Auditory Prosthesis Stimulation

Submitted by:

(in alphabetical order)

Ben Bonham, Ph.D.

John Middlebrooks, Ph.D.

Steve Rebscher, M.A.

Russell Snyder, Ph.D.

University of California, San Francisco

Department of Otolaryngology – Head and Neck Surgery

Epstein Hearing Research Laboratories

533 Parnassus Avenue, Room-U490

San Francisco, Ca 94143-0526

Abstract

This Quarterly Progress Report presents our progress in the third quarter of this contract. During this period, we have made progress in following areas: 1) We have fabricated six additional multi-channel intracochlear implants designed specifically for the guinea pig. 2) These implants incorporated several alternative design features and we have tested the effects of these design features on activity evoked in the auditory system. We have conducted 23 physiological experiments in acutely deafened guinea pigs to test the effects of different contact sizes and contact configuration on the distribution and threshold of evoked activity in the central nucleus of the inferior colliculus (ICC). 3) During the first phase of several of these experiments, prior to deafening of the animals, we have continued our studies of acoustic simulations of channel interaction in intracochlear electrical stimulation (ICES) using two-tone interactions in a forward masking paradigm. These experiments are designed to model certain aspects of channel interaction occurring when two electrical channels are activated non-simultaneously. These acoustic simulation experiments provide a basis for comparison with ICES channel interactions, especially in the case of forward masking of pulse trains on one channel by those on another channel. The preliminary results of these acoustic experiments will be presented at the Society for Neuroscience Meetings in October (Bonham et al, 2003a). 4) In the second phase of each of these experiments, we have examined electrical channel interactions using our multichannel guinea pig implant implants activated with pulse trains. Many of these experiments were conducted in collaboration with Dr. John Middlebrooks, who spent the summer in our lab. Preliminary results from these experiments were presented at the recent Conference on Auditory Prostheses at Asilomar in August (see Middlebrooks et al, 2003 and Bonham et al, 2003). These and subsequent results will be presented at the ARO meeting in February. 5) We have directly compared recordings obtained using two different multichannel data acquisition systems: those obtained using our custom 16-channel data acquisition system and those obtained using Dr. Middlebrooks' commercial data acquisition sytem. Our system is based on specially fabricated hardware. Dr. Middlebrooks' system is based on the Tucker-Davis "Medusa" hardware. Both systems require custom software. We obtained recordings using both systems in the same animals using the same recording probes located at the same ICC recording depths. We are comparing the data recorded with these systems in order to determine their relative merits with respect to several critical features including artifact rejection, stability and speed of data acquisition. Each of these systems is being considered as a basis for our projected 32-channel data acquisition system, a system that is required for carrying out experiments in larger animal models, including cats and monkeys, comparable to those conducted in guinea pigs and described in our publications and progress reports. Cats and monkeys have larger brains and larger inferior colliculi. Therefore, probes with larger numbers of recording contacts are required to sample the distribution of evoked neural activity across them with the same spatial resolution. 6) We have completed and submitted for publication a manuscript, which describes the results of our initial ICES experiments using the 16-channel recording probes and single channel stimulation. These experiments describe the basic response properties of inferior colliculus (IC) neurons in guinea pigs to single tones and single ICES pulses recorded with the 16-channel probes (see Snyder et al, submitted).

Fabrication of Guinea Pig Intracochlear Stimulating Implants

As described in previous quarterly progress reports, we have designed an intracochlear stimulating implant to fit the specific dimensions and shape of the guinea pig (GP) cochlea (Figure 1). Our goal is to design a flexible research tool that will allow multichannel electrical stimulation producing with as many as six non-overlapping regions of excitation in the auditory nerve array. We anticipate that by using an optimum combination of implant contact sizes, contact configurations (monopolar, bipolar or tripolar) and stimulation strategies (monophasic, biphasic, or pseudomonophasic), we will be able to manufacture implants that will allow us to reliably activate up to 6 sectors of the auditory nerve array in the four octaves between 2 and 40 kHz at 6 dB above threshold.

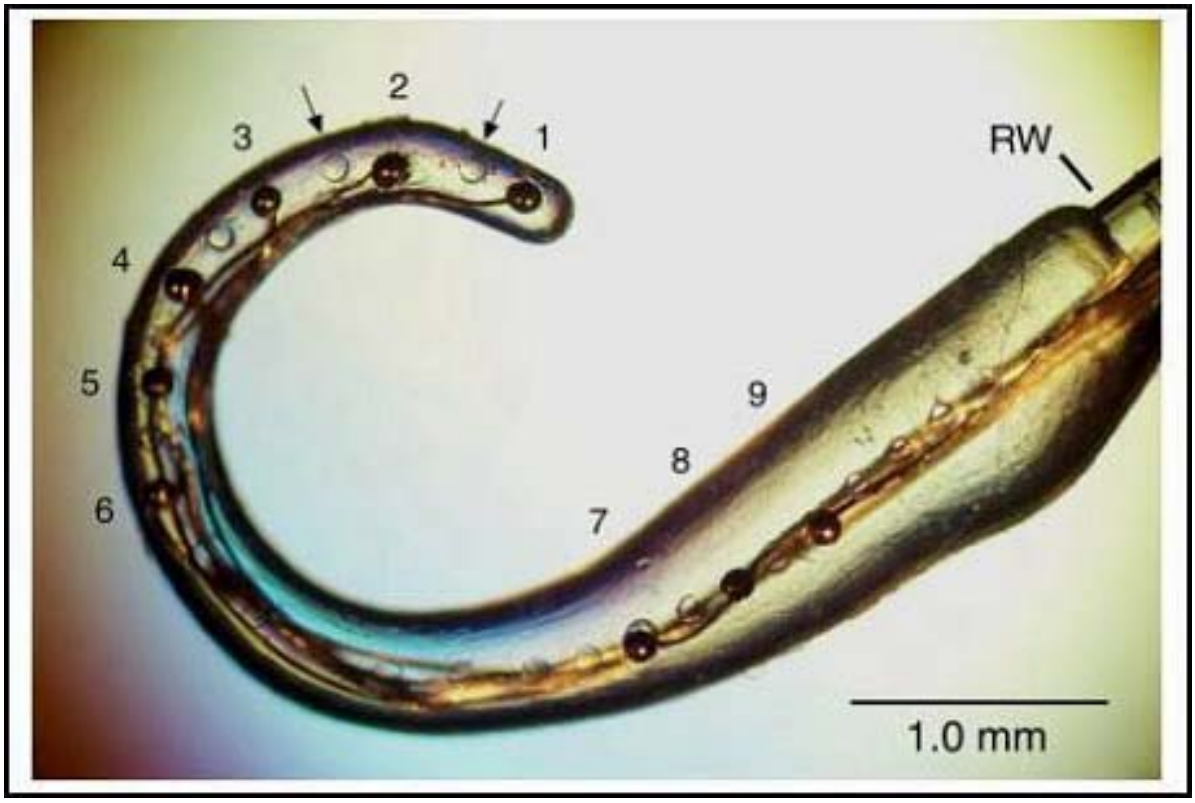

Figure 1. The first GP implant was fabricated with sets of contacts: 6 contacts (1-6) located near the apical tip of the implant, 3 contacts (7-9) located nearer the implant base. The spacing between contact centers within each set was 500µm, the diameter of each contact was 175µm. A space of 2.25 mm separates the apical and basal sets. The current dye has contact-placement dimples that allow contact ball to be precisely placed at any of 27 longitudinal locations along the carrier. The arrows indicate two of the unused contact-placement dimples (see QPR#2) at locations between the three most apical contacts. RW indicates the anticipated location of the annulus of the round window.

Our first implant design (Figure 1) consists of a clear silicone rubber carrier and nine insulated Platinum/Iridium (90%:10%) wires 0.001" in diameter. The ends of these wires were flamed into ball contacts 175µm in diameter. These nine contacts are arrayed as two

sets of contacts, a basal set of three contacts (#7-9), and an apical set of six contacts (#1-6), arrayed in longitudinal series along the length of the intracochlear portion of the carrier. The separation between the nine contacts within each set is 500µm and the diameter of all contacts is 175µm. In our subsequent designs, the implants have contacts with various intercontact spacings (250 - 750µm); some implants have contacts with larger diameters (300µm); and some have contacts arranged in radial as well as longitudinal configurations

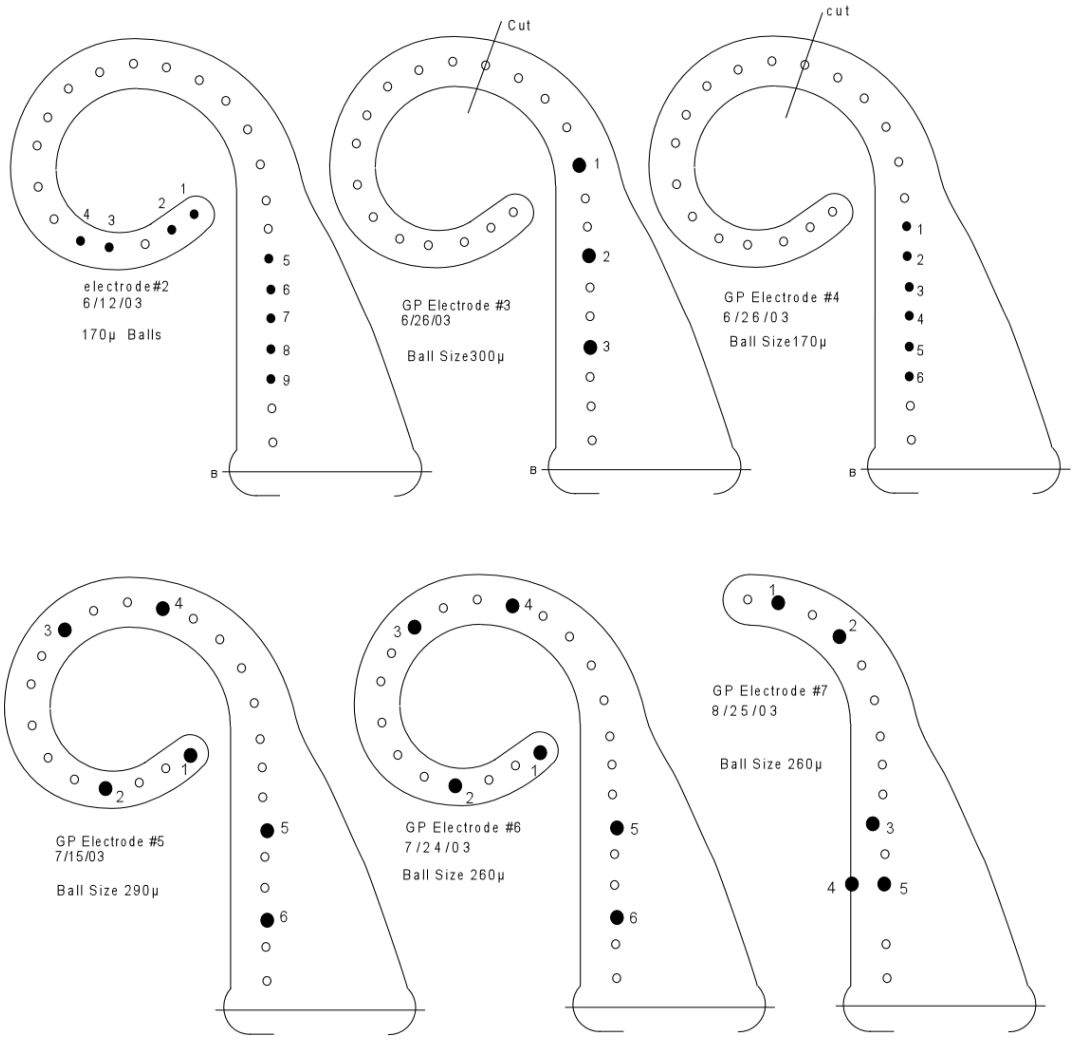

Figure 2. Diagrams of the six GP implants fabricated using the current mold during this period. Three of these implants (#3, #4 & #7) were truncate at the tip to allow easier insertion and re-insertion into the scala tympani. Implants #2 & #3 were fabricated with 175µm contacts. The remaining four implants were fabricated with 300µm contacts.

The subsequent six designs are diagrammed in Figure 2. We have fabricated implants with a range of designs in order to test the effects of contact location, separation (for bipolar and tripolar stimuli), and size on the activation patterns (see Figures 5 & 6 &7) evoked by these implants. With our multichannel recording probes, we have also examined the amplitude of

the electrical artifacts produced by activating these contacts in various configurations (see Figures 6 & 7). Our goal is to identify those design features and stimulation strategies that evoke the most selective excitation at the lowest thresholds with the smallest amount of electrical artifact. As these features are defined, we plan to incorporate them in implants that will selectively excite the auditory system and produce true multichannel stimulation.

Effects of Implant Designs and Stimulation Strategies on ICES Selectivity and Threshold.

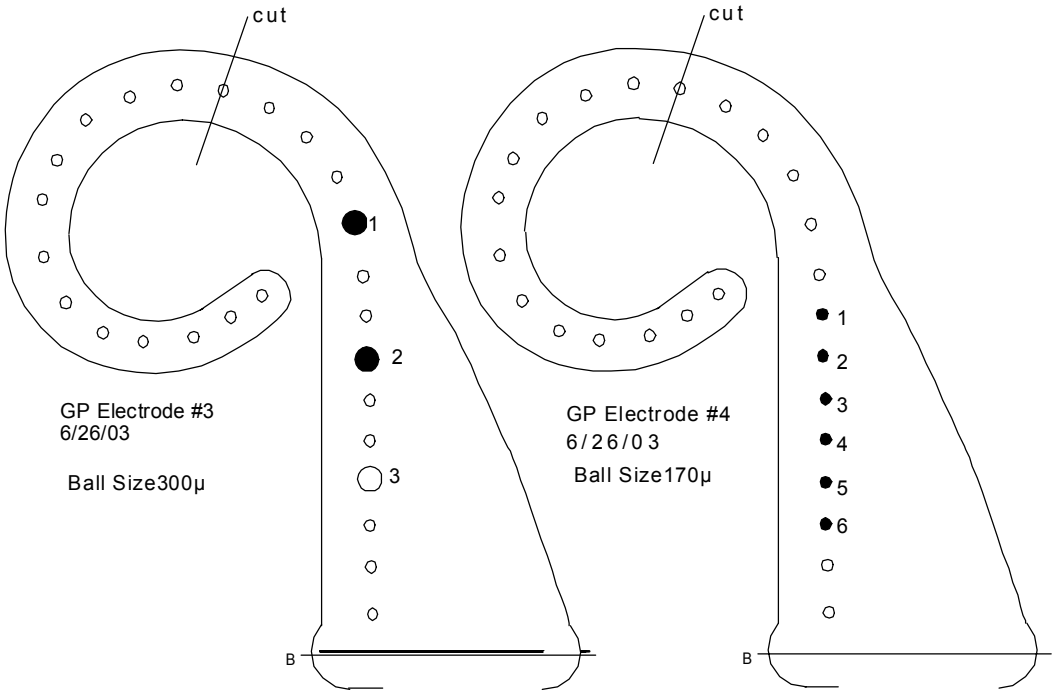

Figure 3. Two intracochlear implant designs that were inserted into the scala tympani of guinea pig 36. The stimulation contacts in implant #3 (left) are almost twice the diameter of the contracts in implant #4 (right). The responses evoked by stimulation of these two implants were directly compared using the same recording probe inserted into the IC of this animal and fixed in place prior to deafening the animal and insertion of either implant.

An example of two different implant designs is illustrated in Figure 3. These designs use the same basic guinea pig carrier but incorporate two different design features. Implant #3 (E3) consists of three wires ending in large contacts, 300 µm in diameter. The contacts are widely separated by a distance of 750 µm. Implant #4 (E4) consists of six wires ending as small contacts separated by the minimum distance our implant mold currently allows, 250 µm. The tips of each of these implants were cut off to allow easy insertion, removal, and re-insertion into the scala tympani of a single guinea pig. In experiments employing these implants, a recording probe was inserted into the IC and calibrated using acoustic tones (Figure 4). Tones at a range of frequencies and intensities were presented to the cochlea and the frequency response areas at each recording site were constructed. Characteristic frequencies (CF's) were estimated for each site by estimating the frequency that evoked a response at the

lowest intensity for that site. In Figure 4, there is a clear shift in CF from low to high frequencies as one moves from the most superficial site (upper left) to the deepest site (lower right). The estimated CF at each site is used to calibrate the recording probe. These CF's are shown in following figures on the right ordinate of electrically evoked spatial tuning curves (STCs).

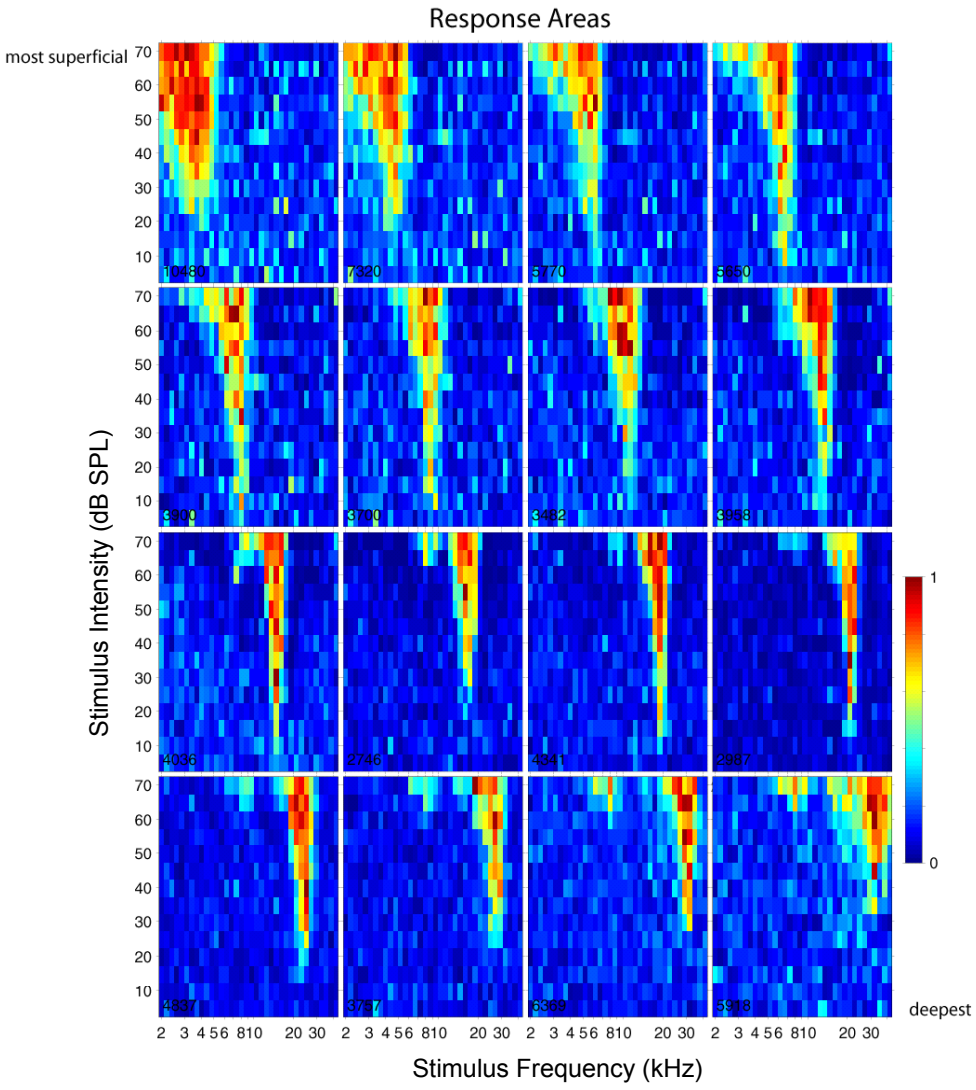

Figure 4. Frequency response areas (FRAs) recorded before deafening and insertion of the intracochlear implant. Each panel represents acoustic responses recorded at one recording probe site to tones varying in frequency from 2 to 42 kHz and level from 5 to 70 dB SPL.

After the recording probe was inserted and fixed in place, the animal was deafened using an intracochlear injection of neomycin sulfate. When the animal became deaf, intracochlear stimulation implant #3 was inserted into the cochlea and electrical stimuli were used to activate selected contracts on this implant. After these responses were recorded, implant #3 was removed and implant #4 was inserted into the cochlea and the process repeated. The spread of activity in across the auditory nerve array evoked by

activation of these implants was estimated by measuring the distribution of activity evoked by across this calibrated probe using STCs.

Effects of contact size and separation on threshold, spatial tuning and artifact production: Figure 5 illustrates two representative STCs evoked by the two different intracochlear implants. In this instance, the recording probe had two non-functional sites, one at a depth of 1300 and the other at a depth of 1500 microns (corresponding to sites #14 & #11 respectively of this probe). Nevertheless, cochlear stimulation using these two implants evoked comparable responses at the remaining probe sites. The STC on the right, evoked by bipolar pulses on pair 1,2 of E3 (the implant with the larger and more widely spaced contacts), is slightly narrower, has slightly higher spatial selectivity, and has significantly lower minimum threshold than the STC on the left, which was evoked by the same pulses on pair 1,2 of E4 (smaller, more closely-spaced contacts).

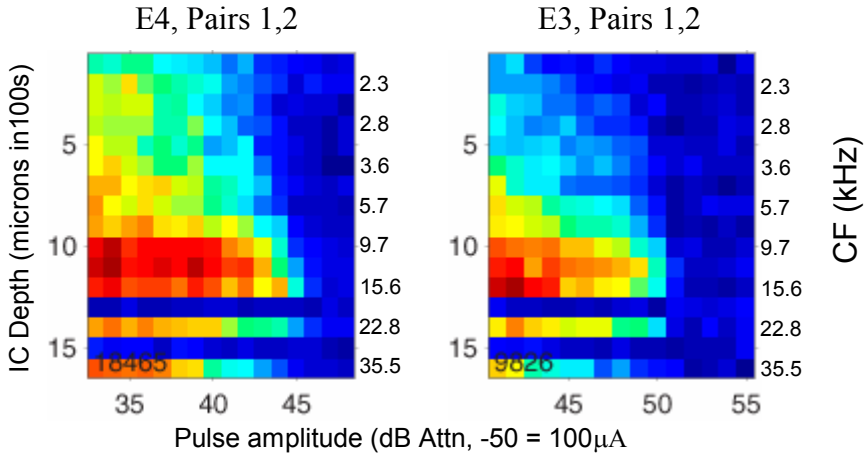

Figure 5. Representative spatial tuning curves (STCs) evoked by bipolar stimulation of sites <1,2> of implants #s 3 & 4. Recording probe site numbers are listed on the left ordinate. The estimated CF is indicated on the right ordinate. The abscissa indicates the pulse amplitude. Data from gp36_10 & gp36_18.

Thus these two implant designs do not evoke dramatically different excitation patterns in the ICC even though the separation between the bipolar contacts of one (E3) was 3 times that of the other (E4). These results are surprising given our previous results examining the effects of implant contact separation. We plan to examine the effects of contact separation in more detail in the coming quarter.

In contrast to the spread of activation evoked by E3 and E4, the analogue waveforms they evoke are significantly different. Figure 6 illustrates an example of the analogue waveforms evoked by two bipolar pulses separated by 50 ms applied to contact pair <1,2> of E4 (the implant with the small contacts). These pulses were applied at a level 3 dB above the minimum level required to evoke a neural response. At this level, the pulses evoked small neural responses at some sites and a large electrical artifact (occurring at 200 samples and 120 samples, 10 ms and 60 ms respectively, after the recording began) at most recording sites. The lone exception is site 14 at which no neural response could be observed using any stimulus at any level. At all the remaining recording sites and at all stimulus levels, the electrical artifact was as large as or larger than the evoked neural responses.

Thus electrical pulses on E4 evoked neural activity, but they produced large artifacts. In this case, detecting the neural responses using these pulses was not difficult even in the presence of such large electrical artifacts. When the pulses are brief and separated by at least 10 ms, the 5-10 ms latency between the artifact and the neural responses allows them to be easily separated. When the pulses are more closely spaced, the electrical artifact of one pulse partly obscures the neural response to the previous pulse. Thus, when pulse rates greater than 100 pps are used with implants like E4, electrical artifacts present a recording problem. This problem becomes acute in experiments that are designed to simulate human CI stimulation, where rates greater then 500 pps are commonly used.

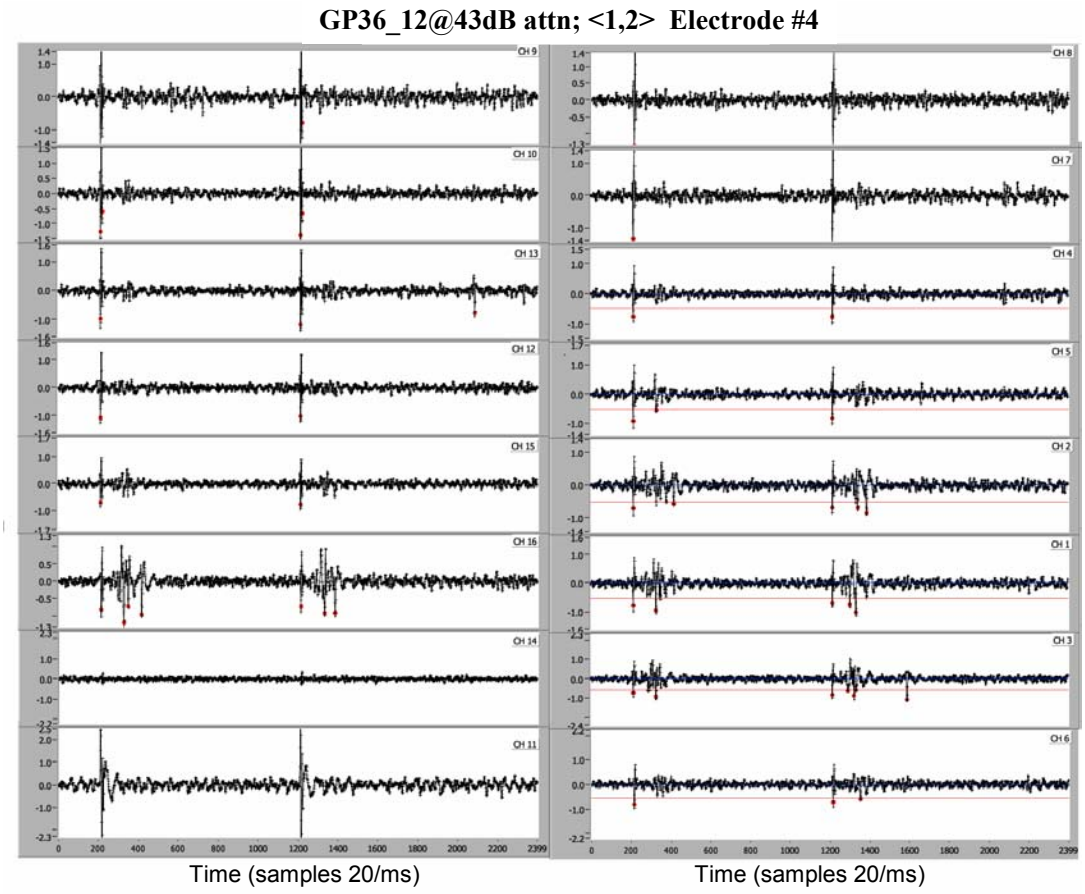

Figure 6. Analogue waveforms evoked by bipolar activation of contact pair <1,2> of implant #4. These small contacts were activated using two biphasic pulses (0.2 ms/phase) separated by 50 ms at -43 dB attn, 3 dB above threshold.

There are several strategies for dealing with electrical artifacts in the recordings of the neural responses, including on- and off-line filtering, blanking, and subtraction. Perhaps the most straightforward strategy, however, is illustrated in Figure 7. This figure illustrates comparable analogue waveforms evoked by implant contact pair <1,2> of implant E3, an implant which had larger stimulation contacts and lower impedances. All stimulus and recording parameters in this recording are identical to those used in the previous recording with E4. It should be noted, however, that the pulse amplitude (-43 dB attn), identical to

that used in Figure 6, is approximately 5 dB higher relative to the neural threshold that was obtained using this implant. Thus, though the stimulation level is higher relative to the neural threshold, the stimulus artifact is smaller. Indeed, there are no electrical artifacts observable at any of the functional sites of this probe. Site 11, like site 14, was not functional, and no responses

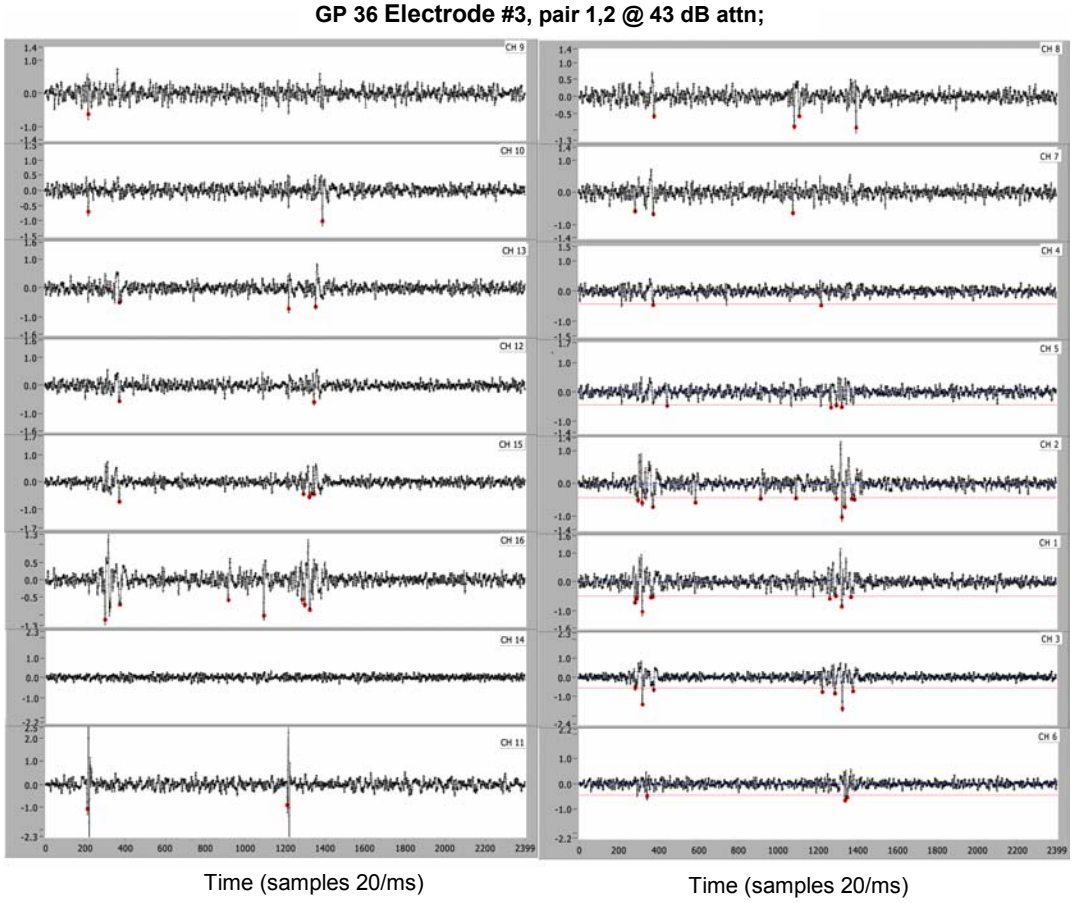

Figure 7. Analogue waveforms evoked by bipolar activation of a contact pair <1,2> of implant #3. The 16 panels illustrate 120 ms of recording on the 16 probe sites. This implant's relatively large contacts were activated using two biphasic pulses (0.2 ms/phase) at 3 dB above neural response threshold.

could be recorded from it. Large neural responses can be seen on all the remaining sites. This suggests that one technique for minimizing electrical artifacts in a physiological recording context is to lower the impedance of the stimulating implant contacts. The results just presented suggest that one way to accomplish this is to use implants with large contacts. "Activation" of iridium oxide deposited on the contacts is another potential technique for reducing contact impedance. We plan to examine the effects of iridium oxide "activation" during the next quarter.

Effects of stimulus waveform on threshold and spatial selectivity: In a series of experiments, we have examined the effects of stimulus waveform on threshold and spatial

selectivity. We have activated the same bipolar implant contact pairs with biphasic pulses and pseudomonophasic pulses (i.e., biphasic pulses with a short excitatory phase and a long recovery phase). We have also examined the effects of reversing the polarity of these pulses so that the cathodic excitatory phase of the pulse is delivered to one or the other contact of a bipolar

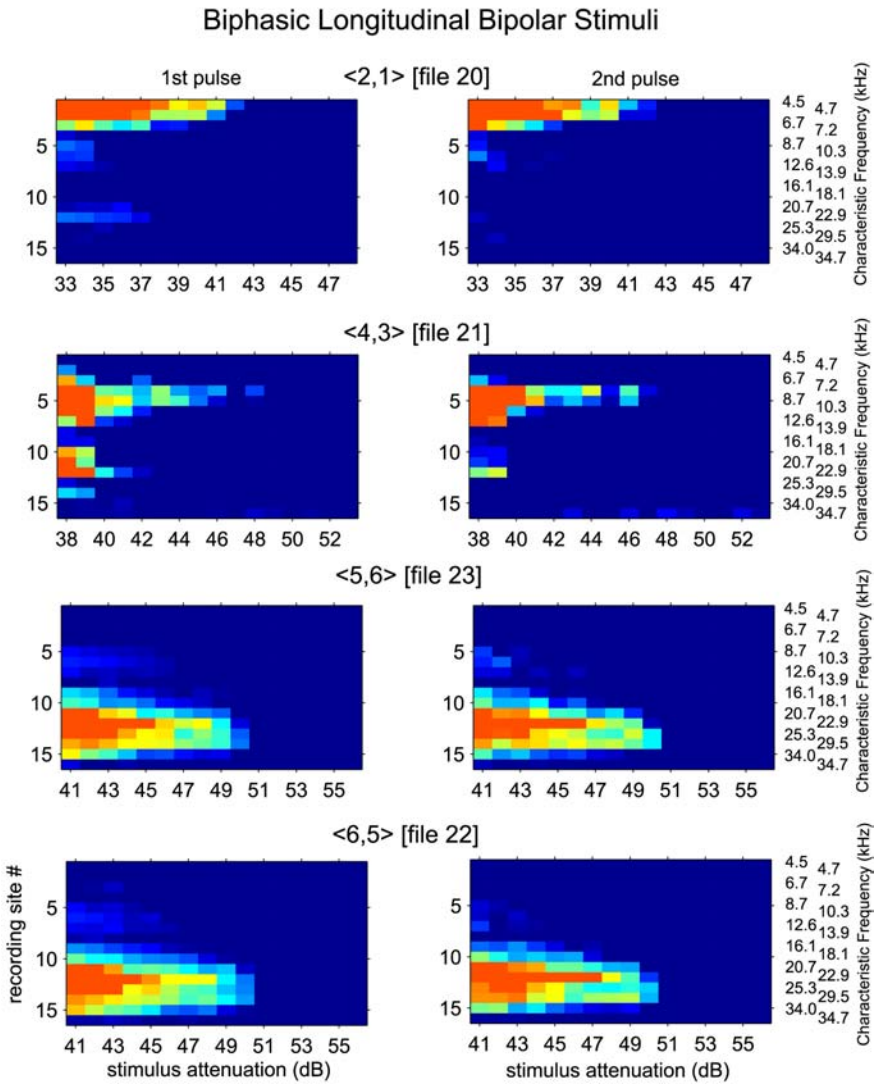

Figure 8. STCs for longitudinal bipolar implants activated with equal phase duration (0.2ms) biphasic pulses. Left ordinate is recording site number (relative IC depth in 100s of microns). Right ordinate is characteristic frequency determined using the acoustic responses illustrated in Figure 4.

pair. Figure 8 illustrates the spatial tuning curves evoked by activation of each of three bipolar contacts. These contacts were activated with normal equal phase-duration biphasic pulses. The excitatory phase was always delivered to the contact listed first in each pair, e.g., for pair <2,1> the cathodic excitatory phase was delivered to contact 2. The STCs for each bipolar pair are illustrated twice, once for each of two independent pulses presented 50 ms apart. There is a clear shift in location of the activity patterns from low to high frequencies as the stimulated contact pair moves basally from the pair

in the 2nd turn <2,1> to middle of the 1st turn <4,3> and finally to the pair at the junction of the basal turn and hook region <6,5>. These STCs are very narrowly tuned with relative low thresholds (100 – 250 μA, -50 dB = 100 μA).

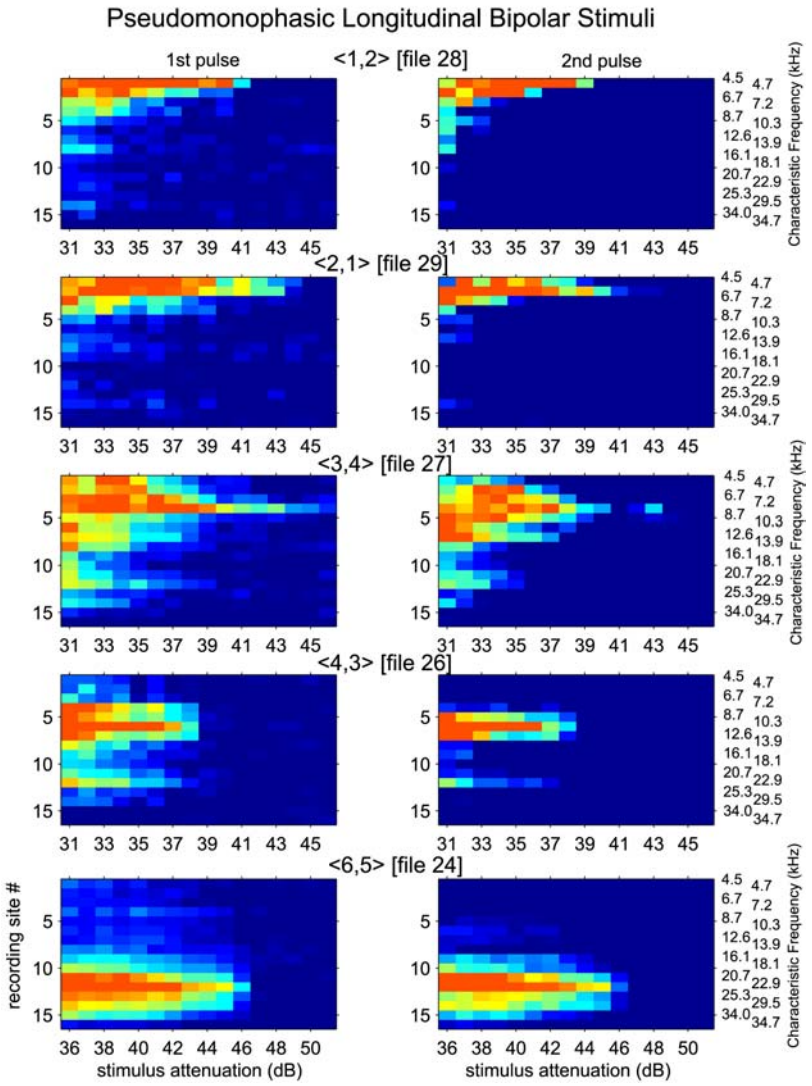

Figure 9. STCs for longitudinal bipolar contacts activated with pseudomonophasic pulses. The ratio of excitatory to recovery phase duration was 1:10. Duration the excitatory cathodic phase was 0.2 ms. Left ordinate is recording site number (relative IC depth in 100s of microns). Right ordinate is characteristic frequency determined using the acoustic responses like those illustrated in Figure 4.

Figure 9 illustrates the spatial tuning curves evoked by the same bipolar contacts activated with pseudomonophaic pulses. The duration of the excitatory cathodic phase of these pulses was 0.2 ms. The ratio of cathodic to anodic phase durations was 1:10. As in Figure 8, the STCs for each bipole are illustrated twice, once for each of two independent pulses. These STCs are even more selective than those evoked by equal-phase pulses illustrated in Figure 8. Moreover, they shift slightly but significantly when the cathodic excitatory phase is shifted from the more apical to the more basal contact of the bipolar pair. These results

suggest that extremely selective activation patterns can be evoked and that they can be position very precisely relatively to one another. We intend to explore this possibility in greater detail in the coming quarter.

Modeling of ICES Channel Interaction Using Acoustic Two-Tone Stimulation

In most CI processors, stimuli on different contacts are presented *non-simultaneously*. Pulses on adjacent or nearby contacts are interleaved so that their electrical fields do not interact. In principal, electrical pulses on different intracochlear implant contacts can excite totally independent sectors of the auditory nerve and evoked activity in non-overlapping regions of the central auditory system. Such non-overlapping activation patterns should produce the smallest amount of channel interaction and this interaction should be the easiest to characterize. Therefore, it is one of our goals to produce and characterize these interactions.

In normal hearing listeners, two-tone stimulation in the forward masking paradigm (in contrast to simultaneous masking) has comparable possibilities, since this paradigm avoids the *spectral* interactions (two-tone suppression, distortion product generation) that normally occur between simultaneous presented acoustic signals. Forward masking has also been used to measure *temporal* interactions of acoustic signals.

Psychophysical studies of temporal interaction in CI users have focused on forward masking and gap detection **within and between** channels to estimate temporal interactions (Tong and Clark, '86; Shannon, '90; Chatterjee et al '98; Hanekom and Shannon, '98; Chatterjee and Shannon, '98; Chatterjee, '98). These studies have estimated temporal integration times (~100 ms) and recovery time constants (50-100 ms) and reported that these temporal measures approximate those observed acoustically. Moreover, they have correlated measures of temporal processing with the speech reception performance and in some cases have reported high correlations (e.g., Chatterjee, '98). In general, these studies have emphasized the similarities between acoustic temporal processing and temporal processing seen during ICES. Therefore, we have examined the response properties of IC neurons in a forward masking paradigm in which a probe tone that is fixed in frequency and intensity is preceded by masking tone that varies in both frequency and intensity.

To examine two-tone interactions in inferior colliculus (IC) neurons, 16-channel silicon recording probes (U. of Mich. CNCT) were inserted into the inferior colliculus central nucleus (ICC) of Ketamine anesthetized adult guinea pigs. Frequency response areas (FRAs) were recorded by presenting 50 ms contralateral tones varying in frequency and level over a range of 4-4.5 octaves and 70-80 dB. After single-tone FRAs were recorded, two-tone FRAs were recorded by presenting a 30 – 50 ms fixed probe tone preceded by a 60 ms variable masking tone. The probe tone was fixed in frequency (usually between 9 and 16 kHz) and in level (presented at a moderately loud level, usually between 50 and 60 dB SPL). The preceding masker tone varied in both frequency (usually between 2 and 40 kHz in 1/8 octave steps) and intensity (usually between 15 and 80 dB SPL in 5 dB steps). The recording duration encompassed the duration of both the forward masking tone and the probe tone, so that by varying the analysis window, responses to either the masker alone or the probe alone or both could be examined.

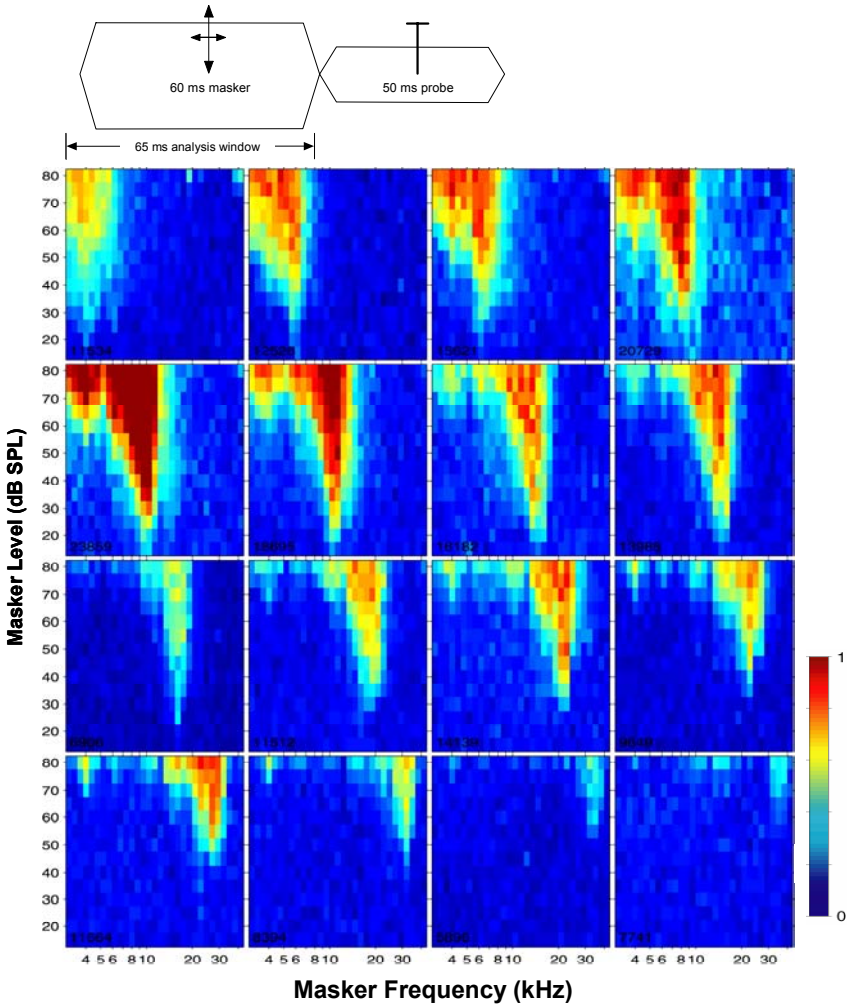

Figure 10. Frequency Response Areas (FRAs) of ICC neurons evoked by forward masking tones, which varied in frequency (3 – 42 kHz) and level (15 – 80 dB SPL). Response magnitudes at frequency/level combinations are scaled from no response (dark blue) to the maximum recorded response (dark red). The panel at the upper left illustrates responses from the most superficial recording probe site: the panel at the lower left illustrates responses recorded from the deepest site. Intermediate panels left to right then top to bottom illustrate responses from intermediate probe sites.

In figure 10, FRAs evoked by the variable masker tones alone are displayed. Since the masker tones precede the probe tone, these are simply FRAs as shown in Figure 4. As in Figure 4, recordings from the most superficial site are represented in the upper left panel; those from the deepest site are represented in the lower right panel. Response magnitudes are scaled as a proportion of the maximum response and color-coded according to the scale on the right. Like the recordings in Figure 4, the most superficial sites are tuned to relatively low frequencies and the deepest sites are tuned to relatively high frequencies.

In figures 11 and 12 are shown the **temporal response patterns** of the same neurons to the same variable frequency masker presented at a *fixed level.* This figure also illustrates the response to the fixed-level, fixed-frequency probe tone. The responses to both masker and probe are plotted as a function of masker frequency (ordinate) and peri-stimulus time

(abscissa). In these panels, the masker response begins at 15 ms and ends at 65 ms; the probe response begins at 70 ms.

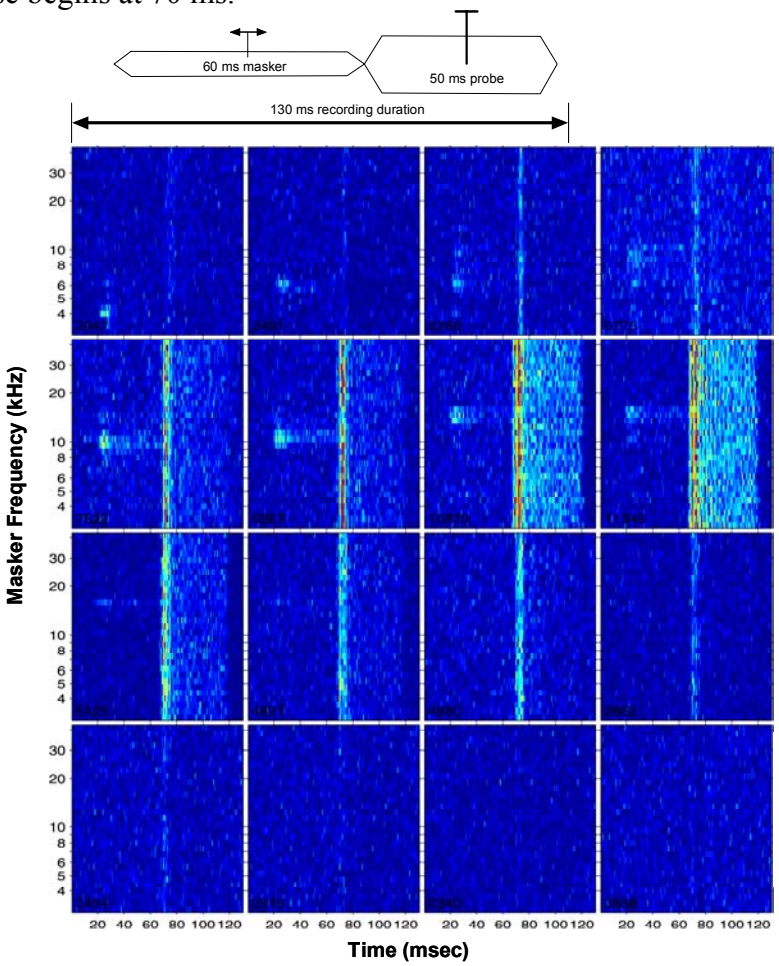

Figure 11. Masker frequency vs. time plots of responses of the same neurons as Figure 10 to the variable-frequency, forward masking tone at a fixed-level (20 dB SPL) and a fixed-frequency, fixed-level probe tone (15 kHz, 45 dB SPL). Each panel represents the response recorded at one recording probe site during the time interval indicated in the diagram above. The order of the panels is identical to that of the previous figure.

In figure 11, the masker level is relatively soft (20 dB SPL) and the probe level is relatively loud (45 dB SPL). As in Figure 10, each panel represents the response recorded at one recording probe site. The 130 ms analysis interval is indicated in the diagram above the figure. Within each panel, the response to the 20 dB SPL variable frequency masking tone is plotted. The masking tone varied from 3-42 kHz in 1/8 octave steps. After each masking tone the response to the 15 kHz, 45 dB SPL probe tone is evident. Since the masking tone is a relatively quiet stimulus, it evokes only a weak response, which can be seen in only the upper 10 panels. In panels 1-10, the centroid of the masker response moves successively as the CF of the neurons recorded in each panel increases. In all the panels, the probe response, which begins at 70 ms, appears as a vertical stripe. In panels where the neurons' CF approximates the probe frequency, the probe response is larger and more sustained (e.g., see panels 7 & 8). In panels where the neurons' CF is above or below the probe frequency, the

probe response is smaller and more of an onset response (see panels 3 & 12). Although it is variable from panel to panel, the probe response is relatively constant within any given panel. From this we can infer that the masker intensity is too low to affect the probe response. The probe response does not vary significantly despite variations in the masker response within and across the panels.

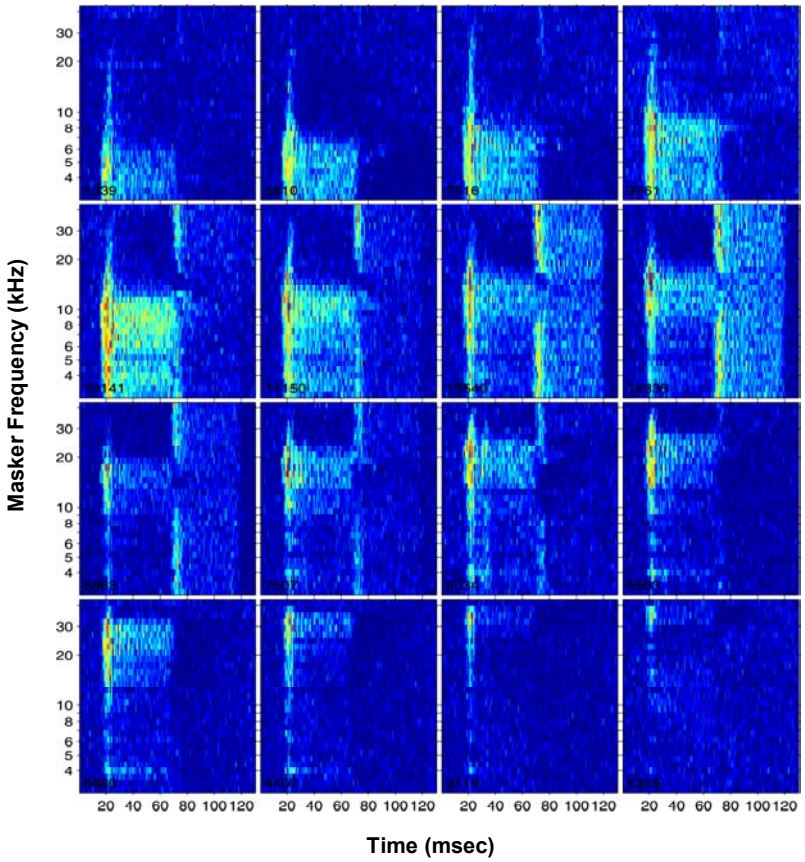

Figure 12. Masker frequency vs. time plots for responses to the same forward masking and probe tones as in figure 4, but the masking tone in this figure is at 75 dB SPL. The organization of the panels is identical to that in the previous figures.

Figure 12 illustrates the responses of the same neurons when the masking tone is relatively loud, 75 dB SPL. In contrast to the 20 dB masker in Figure 11, the masker now evokes a strong response at all recording sites beginning at 15 ms. Just as in Figure 11, since neurons at different sites have different CFs, the centroid of the masker response moves upwards in each successively lower panel even though the same stimuli are presented in all panels. The probe response in this figure is different from that seen in Figure 11, although the probe stimulus is identical.

Whereas the probe response could be discerned in all panels in Figure 11, it is now difficult to see it in several panels. Where it can be seen, it appears as an interrupted vertical stripe beginning as before at 70msec. The size of the interruption in (i.e., masking of) the probe response is variable depending upon site CF (depth within the ICC). In the four upper

panels (most superficial locations), which show responses of neurons tuned to low frequencies, it can be seen only at the top of these panels, after the highest masker frequencies (i.e., those that would be expected to evoke the smallest response at these locations). In the lowest four panels representing the responses of neurons tuned to the highest frequencies, it cannot be seen at all. At the remaining sites, the size of the interruption (degree of masking) is variable. At sites whose CFs approximate the probe frequency, the interruption is relatively small and transient (see panel 8; 2nd row, 4th column). The masker affects primarily the probe onset response. At sites whose CF is slightly above or below the probe frequency, the interruption in the probe response is larger and more sustained (see panels 6 & 10; 2nd and 3rd row, 2nd column). At these locations, the masker suppresses not only the onset response of the probe but also its sustained response. At sites with CFs even further from the probe frequency, the probe evokes only an onset response. However, at these sites a broad range of masker frequencies suppresses the probe onset response. Thus, when the masker intensity is relatively high, as in these recordings, it strongly affects the probe response and this suppression varies with time, masker frequency, masker intensity and site location (CF).

This variation in suppression with site location is illustrated in Figure 13. This figure shows FRAs of same ICC neurons when the analysis window is restricted to the first 10 ms of the fixed-frequency, fixed-level probe tone used in the previous two figures. Thus, in this figure the only signal present during the recording interval is the fixed frequency/intensity probe tone. The organization of the panels in this figure is identical to that in the previous figures. If the masker had no effect on the probe response, each panel would be a noisy rectangles relatively uniform in color. Instead, the probe responses in each panel show a clear pattern of suppression that varies dramatically as a function of the masker level and frequency. In many cases, the probe response is suppressed completely by the masker and appears as a negative image of part of the masker response at that location. Compare, for example the masker response at site 8 in Figure 10 with the probe response at the same site in Figure 13. This comparison suggests that the suppression of the probe response can be in part the result of adaptation of these neurons to the masker tones. In other cases, the frequency/intensity region of probe masking is dramatically different from the masker response (i.e., the FRA). For example, compare the masked probe responses at sites 1 & 5 in Figure 13 with the corresponding masker responses in Figure 10. At site 1, the masker response is centered at 4 kHz and extends up to about 6 kHz. In contrast, suppression of the masked probe response at this site is centered at about 15 kHz, and may not reach as low as 6 kHz. Thus the masker excitation and suppression do not overlap. At site 5, the masker evokes strong excitation that is centered at approximately 10 kHz but extends broadly from just above 15 kHz to below 3 kHz. In contrast, masker suppression of the probe response occurs across an extremely narrow range of frequencies centered at 15 kHz and extending from about 12 kHz

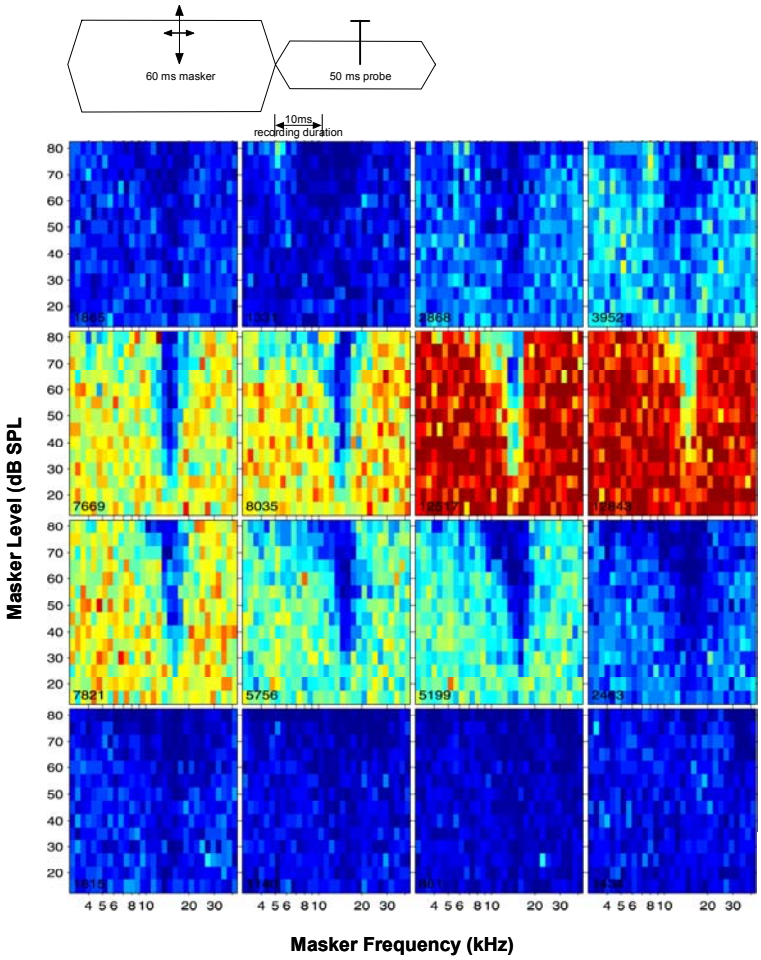

Figure 13. Responses of same ICC neurons illustrated in the previous three figures to the first 10 msec of the same fixed frequency probe tone, 15 kHz @ 45 dB SPL. The organization of the panels in this figure is identical to that in the previous figures. The duration of the recording interval is indicated in the diagram above the figure.

to just above 20 kHz. Thus at this site the excitation and suppression overlap, but their frequency spreads are dramatically different. These results indicate first that the suppression of probe response varies dramatically not only with time, masker frequency and masker intensity, but also with IC location. Second, they indicate that the suppression of the probe response is often not directly related to the intensity of the masker response, i.e., that it is not related to the number of spikes evoked by the masker. This lack of correspondence between masker response and probe response suppression strongly suggests that the probe suppression is the result of inhibition rather than adaptation. The variations in correspondence between masker and probe response locations, in turn, suggests that channel interactions among intracochlear electrical stimuli will vary depending upon the frequency separation between the electrically stimulation sectors of the auditory nerve.

In the next quarter, we plan to continue to investigate the interactions between acoustic tones to provide a model and guide for our investigation of the interactions of electrical channels. We plan to continue our forward masking experiments and to extend our non-simultaneous masking experiments by looking at the interactions of interleaved

gamma tones as a model of interleaved electrical pulses. Meanwhile, we plan to summarize our acoustic forward masking results in a draft manuscript that we will submit for publication.

Forward Masking using ICES – A Model of Electrical Channel Interaction

During this quarter, we have begun an examination of electrical channel interactions using our multichannel guinea pig implants activated with pulses and pulse trains in a forward masking paradigm. Many of these experiments were conducted in collaboration with Dr. John Middlebrooks, who spent the summer in our lab. These experiments were designed to mimic as closely as possible the acoustic forward masking described above.

In most of these experiments we used a forward masker consisting of a 100 ms pulse train consisting of 0.2 ms/phase biphasic pulses delivered at 250 pps. This forward masker was followed by a 20 ms probe pulse train consisting of identical pulses delivered at the same frequency. The probe and masker signals varied in level relative to one another and were delivered either on the same implant contact pairs or on contact pairs separated by various distances.

Publications:

Snyder, R.L., J.A. Bierer, J.C. Middlebrooks. (2003) Topographic spread of inferior colliculus activation in response to acoustic and intracochlear electrical stimulation. J. Assoc. for Research in Otolarlyngol. In press.

Middlebrooks, J.C., R.L. Snyder, J.A. Bierer. (2003) Effects of Scala Tympani Electrode Configuration on Spread of Activation in Inferior Colliculus. Conference on Implantable Auditory Prostheses. Asilomar, California.

Bonham, B.H., R.L. Snyder, S.J. Rebscher, J.A. Bierer. (2003) Effects of single and multichannel stimulation on spread of activation in the inferior colliculus using a UCSF-type scala tympani electrode. Conference on Implantable Auditory Prostheses. Asilomar, California.

Bonham, B.H. R.L. Snyder, J.A. Bierer. (2003) Two-tone channel interaction in the inferior colliculus. Society for Neuroscience Abstr.

Work Planned for the Next Quarter

1) We will begin experiments looking at channel interaction using electrical stimulation. We will attempt to correlate the spread of excitation as defined by spatial tuning curves in the IC with the spread of excitation as defined by reduction of EABR amplitude using inter-pulse intervals between 4 and 50 msec.

2) We will begin experiments employing implants with closer contact spacing between contacts. Our current implant uses a minimum spacing of 500 μm between contacts. In the next quarter we will fabricate an implant in which at least some contacts have a minimum spacing of 250 μm.

3) Work will continue on the acoustic model of channel interaction. We will quantify the spread of stimulus inhibition using a non-overlapping two-tone (forward masking) paradigm. We will define the time course of the inhibition by varying the gap between the end of the first tone and the beginning of the second tone. We will define the development of the interaction by varying the duration of the first tone. Finally, we will estimate the relative magnitude of the interaction by varying the intensity of the second tone.

4) Experiments will be continued to look at the effects of implant contact configuration on single channel and multi-channel stimulation. We will examine the spread of excitation using tripolar as well as bipolar and monopolar configurations.